*Int.J.Curr.Microbiol.App.Sci* (2019) *8*(11): 2000-2025

*International Journal of Current Microbiology and Applied Sciences*
***ISSN: 2319-7706* Volume 8 Number 11 (2019)**
Journal homepage: http://www.ijcmas.com

**Original Research Article** https://doi.org/10.20546/ijcmas.2019.811.234

# Evaluation of Antimicrobial Activity of ZnO Nanoparticles against Foodborne Pathogens

**Anjie Jamal[1*], Ramadan Awad[1] and Hoda Yusef[2]**

*[1]Department of Biological Sciences, Faculty of Science, Beirut Arab University, Lebanon*
*[2]Department of Botany and Microbiology, Faculty of Science, Alexandria University, Egypt*

**Corresponding author*

**Keywords**

ZnO Nanoparticles, Antimicrobial activity, Foodborne pathogens

**Article Info**

***Accepted:***
17 October 2019
***Available Online:***
10 November 2019

**A B S T R A C T**

Nanostructures have a great potential in the area of food packaging. This study aims to determine the antimicrobial efficacy for zinc oxide (ZnO) nanoparticles (Nps), compared to bulk ZnO powder. ZnO Nps were synthesized using; co-precipitation and high-speed ball milling method. The synthesized powders were characterized by X-ray diffraction (XRD), Transmission Electron Microscope (TEM), Fourier Transform Infrared Spectroscopy (FTIR) and Ultraviolet-Visible Absorption Spectroscopy (UV). All data revealed the formation of pure nano-sized ZnO. ZnO Nps showed notable size and concentration-dependent antimicrobial effects. In comparison to nanosuspension, the antimicrobial activity of bulk ZnO was almost negligible, a strong significant difference was noticed between the antimicrobial activity of the bulk and that of prepared Nps ($p<0.05$). ZnO Nps exhibited a privileged ability to suppress the growth of foodborne pathogens in culture media and milk samples. Among the bacterial strains tested, Gram-positive bacteria were more sensitive to ZnO nano-treatments. The examination of DNA of *Bacillus subtilis* treated with ZnO Nps using gel electrophoresis, displayed a reduction in band size but the absence of DNA fragmentation. Transmission Electron Microscope illustrated remarkable damages in the cell wall and cytoplasmic membrane of *Bacillus subtilis* cell structure upon exposure to ZnO Nps.

## Introduction

Nanoparticles (Nps) are particles that range in size from 1 to 100 nm. The high surface area to volume ratio provides Nps with quirky properties compared to its bulk form (Buzea *et al.*, 2007). Nanostructures are predominantly categorized into organic and inorganic Nps, the last have received extraordinary attentions due to its ability to tolerate destructive processing conditions, controlled safety and extended shelf life (Stoimenov *et al.*, 2002; Sawai, 2003; Wang, 2004). Among the inorganic Nps, ZnO Nps are semiconductors with a direct wide band gap (3.3 eV) near UV spectrum (Wang, 2004; Schmidt-Mende *et al.*,

2007). Several methods have been approved for the synthesis of ZnO Nps such as high-speed ball milling method, co-precipitation method, sol gel method, hydrothermal technique, vapour phase strategy, mechano-chemical procedure (Manna, 2012). The synthesized nano–powders are highly influenced by the physical and chemical parameters chosen for the synthesis procedure such as the solvent type, temperature, pH and the precursors used (Sirelkhatim *et al.,* 2015). ZnO Nps are alluring due to their broad-ranging applications in diverse fields. ZnO is categorized as a substance generally recognized as safe (GRAS) by Food and Drug Administration of the United States of America (21CFR182.8991) (Saldami *et al.,* 1996). ZnO Nps have gained remarkable attention worldwide due to their surprising antimicrobial activity against pathogenic bacteria and fungi (Jasim, 2015; Díez-Pascual *et al.,* 2018). Recently, ZnO Nps also proved to exhibit a significant anti-biofilm activity against wide variety of microorganisms (Khan *et al.,* 2014; Shakerimoghaddam *et al.,* 2017; Bhattacharyya *et al.,* 2018). Although the exact antimicrobial activity for ZnO Nps is still unclear (Shi *et al.,* 2014; Sirelkhatim *et al.,* 2015; Arciniegas-Grijalba *et al.,* 2017). Previous studies proposed various mechanisms such as: release of reactive oxygen species (Sawai *et al.,* 1998; Jones *et al.,* 2008; Jalal *et al.,* 2010), release of zinc ions (Reddy *et al.,* 2007; Padmavathy and Vijayaraghavan, 2008), electrostatic interaction (Brayner *et al.,* 2006; Zhang *et al.,* 2007; 2008), and the penetration of ZnO nano-structures across the microbial membrane (Navarro *et al.,* 2008; Zhang *et al.,* 2008). As marked, the mechanism of action of ZnO Nps occurs mainly through the direct contact with the microbial cells, which increases the prospect that Nps would be less prone than antibiotics to promote resistant bacteria (Beyth *et al.,* 2015).

The antimicrobial achievements for ZnO Nps against foodborne pathogens prompt its application in food packaging and in food industry. The diffusion of ZnO Nps from packaging material into the surface of food can save food from spoilage, thus prolong the shelf life of food products (Azeredo, 2013). In addition to the antimicrobial activity of ZnO Nps, these nano-structures proved to enhance the mechanical strength, barrier properties and stability of the packaging materials (Shi *et al.,* 2014).

The aim of the present study is to evaluate the activity of ZnO Nps against some bacterial and fungal pathogens, referring to their effects on the growth and structures of the tested microorganisms.

## Materials and Methods

### Foodborne pathogens

Eleven different foodborne pathogens were obtained from the Microbiology lab in Beirut Arab University; nine bacterial species (*E. coli* O157:H7, *Salmonella* sp., *Enterobacter cloacae*, *Citrobacter freundii*, methicillin resistant *Staphylococcus aureus* (MRSA), methicillin resistant *Staphylococcus epidermidis* (MRSE), *Bacillus subtilis*, *Bacillus cereus* and *Bacillus licheniformis*) and two fungi (*Aspergillus* sp. and *Penicillium* sp.). They were used for the assessment of the antimicrobial activity of ZnO Nps.

### Preparation of ZnO Nps

### Preparation of ZnO Nps by co-precipitation method

ZnO Nps were prepared by co-precipitation method (Ahamed and Kumar *et al.,* 2016); 1 M zinc chloride ($ZnCl_2$, 99.9%, Sigma Aldrich), 4M sodium hydroxide (NaOH) and distilled water ($H_2O$) as dispersing solvents

were used to prepare ZnO Nps. 1M $ZnCl_2$ was prepared by dissolving 20 g of $ZnCl_2$ into 146 ml $H_2O$. The obtained solution was then magnetically stirred at room temperature.4 M NaOH was added dropwise to different aliquots of the solution to adjust their pH to 10, 11, 12 and 13 (namely P1, P2, P3 and P4, respectively). The stirring was extended for 2 hours at 60°C. Afterwards, the resultant powder was washed thoroughly with distilled $H_2O$ until the pH decreased to neutral range (pH=7) (Parthasarathi and Thilagavathi, 2011) and then dried at 100°C for 18 hours. Finally, the dried ingots were separated and heated at 550°C for 5 hours yielding ZnO Nps.

## Preparation of ZnO Nps by high-speed ball milling

The starting material purchased ZnO (99.99%, Fluka) of high purity. The milling was carried out for the dry sample in Retshch ball mill machine at 200 rpm with the aid of ceramics balls, the mass of the balls was five times the mass of the powder. Pure ZnO powder was ball milled at different time intervals: 15, 30, 45 and 60 minutes (namely M1, M2, M3 and M4, respectively). Each 15 minutes few grams of ZnO were taken out for characterization.

## Characterization of ZnO Nps

The obtained nano-powders were characterized by X-Ray powder diffraction measurements at room temperature using Bruker D8 advance powder diffractometer with Cu-$K_\alpha$ radiation ($\lambda$ = 1.54056 Å) in the range $25° \leq 2\theta \leq 75°$. The particle size and the morphology of the prepared Nps were determined using the Joel Transmission Electron Microscope JEM-100CX. FTIR analysis of prepared ZnO Nps was carried by Thermoscientifc-Nicolet is5-id1 transmission. UV-Visible measurements were executed using the ultraviolet-visible near the infrared (NIR) spectrophotometer V-670, the absorption edge was observed in the range of 300 - 500 nm at room temperature.

## Preparation of ZnO nanofluid

The stock ZnO nanofluid (2 mg /ml) was prepared using deionized water in a glass beaker with the help of a magnetic stirrer. Once particles were distributed uniformly, the solution was ultrasonicated for 5 minutes in order to suppress agglomeration (Vani *et al.,* 2011). The nanofluid prepared was autoclaved at 121 °C for 15 minutes and then tested its antimicrobial activity after cooling down to the room temperature (Zhang *et al.*, 2007).

## Inocula preparation and standardization

### Preparation of bacterial suspension

Inoculum preparation was done by transferring fresh colonies grown overnight on Müller-Hinton agar plate to 0.85% normal saline. Mcfarland standard (0.5) was used to compare visually the turbidity of the test suspension and adjust it to 1.5 $\times 10^8$ CFU/ml (Madigan *et al.,* 2006).

### Preparation of fungal suspension

Fungal inocula were prepared by growing the isolates on Sabouraud Dextrose agar slants. The slopes were flooded with sterile 0.85% normal saline and the suspensions were adjusted spectrophotometrically (A530 nm) to optical densities that ranged from 0.09 to 0.11. Thus, inocula were ranged from 0.4 x $10^6$ to 5 x $10^6$ CFU/ml (CLSI, M51-A, 2010).

## Antimicrobial Susceptibility Test (AST)

### Disc diffusion method

Stock suspension of bulk and nano-ZnO prepared by the two mentioned techniques were tested for their antimicrobial activities by

the disc diffusion method. The bacterial and fungal inocula were swabbed on the surface of Müller-Hinton and Sabouraud dextrose agar plates, respectively. Sterile filter paper discs soaked with 15 µL ZnO stock solution were placed on the inoculated surface of the culture media. The plates were incubated at 5-8°C for 2-3 hours to permit good diffusion. Then, the plates inoculated with bacteria were incubated at 35±2°C for 16-18 hours and those inoculated with fungi were incubated at 30°C for 72 hours. The experiment was made in triplicate and the mean diameter of inhibition zones were measured in millimeter.

Vancomycin was used as a positive control for *Staphylococcus* species, whereas; ciprofloxacin was used as a positive control for the other bacterial strains. Clotrimazole was used as positive control for fungi. The results were interpreted according to the Clinical and laboratory Standard Institute (CLSI, M51-A, 2010; CLSI, M02-A11, 2012).

## Broth micro dilution Method

### Determination of minimum inhibitory concentration (MIC) and minimum bactericidal concentration (MBC)

Bacterial strains were tested for their susceptibility to ZnO Nps using broth micro dilution method in 96 well plates (CLSI, M07-A9, 2012). Different concentrations of ZnO nano-suspension were prepared using sterile Müller-Hinton broth; 50 µl were introduced to each well and inoculated with 50 µl diluted inocula equivalent to $1\times10^6$ resulting in final inocula equivalent to $5\times10^5$ CFU/ml.

The plates were then incubated for 16 to 20 hours at 35±2°C. The minimum inhibitory concentration (MIC) was determined as the lowest concentration of ZnO Nps that showed no turbidity after incubation. The MBC was the lowest concentration of antimicrobial agent needed to kill 99.9% of the final inoculum (CLSI, M26-A, 1999), and it was determined after broth micro dilution by sub-culturing the content of every well that showed bacterial growth reduction on Müller-Hinton agar plates. The plates were then overnight incubated at 37°C **(**Aamer *et al.*, 2014)**.**The MIC and the MBC were recorded in µg/ml and repeated twice for each tested bacterium.

The MIC index (MBC/MIC) was calculated to confirm whether the action of the investigated antibacterial agent was bactericidal (MBC/MIC <4) or bacteriostatic (MBC/MIC >4) against the bacterial strains tested (Kone *et al.,* 2004).

## Time-kill study

The determination of the killing rate of bacterial strains by a tested antibacterial agent was monitored at different time intervals. Time-kill curve test was done according to the method described in M26-A document of CLSI (CLSI, M26-A, 1999). The test was performed in flasks containing 20 ml of Müller-Hinton broth inoculated with 5 x $10^5$ CFU/ml and supplemented with the desired concentration of ZnO Nps (MIC X 1, MIC X 2 and MIC X 4). The flasks were shaken at 150 rpm at 37 °C (Mirhosseini and Firouzabadi, 2015). To avoid potential optical interference during optical measurements of the growing cultures caused by the light scattering properties of the Nps, the same liquid medium without microorganisms but containing the same concentration of Nps cultured under the same conditions were used as blank controls (Nicole *et al.*, 2008).

## Application of ZnO Nps in a milk sample

Three concentrations of ZnO Nps (MIC X 1, MIC X 2 and MIC X 4) were used as antibacterial treatments in sterile milk

samples. Flasks (50 ml) were inoculated with $5x10^5$ CFU/ml of MRSE or *Bacillus subtilis*; then flasks were shaken at 150 rpm at 37 °C. Sampling for colony counts was done at time zero and after 4, 8, 10, 12 and 24 hours. Serial dilutions were prepared and 20 µl from each dilution was pipetted onto blood agar plates and uniformly spreaded (Peck *et al.,* 2012). Plates were incubated at 37 °C for 24 hours and colonies were counted (CLSI, M26-A, 1999).

## Gel electrophoresis of DNA of *Bacillus subtilis* treated with ZnO Nps

DNA was extracted from *Bacillus subtilis* cells cultivated overnight in a nutrient broth medium at 37 °C for 24 hours in a rotary shaker (150 rpm), medium lacking ZnO Nps was used for the cultivation of control cells.

DNA extraction was carried using Gene Elute Bacterial Genomic Kit according to manufacturer's instructions; the steps of extraction were performed according to the kit Manual. DNA integrity was checked by agarose electrophoresis.

DNA extracts were stained with ethidium bromide and loaded on the agarose gel (1 %). The gel was electrophoresed at 90V for 25 minutes. DNA bands were visualized by a UV light source and documented by ChemiDoc Imaging System.

## Transmission electron microscopy

On the basis of MIC values and time-kill curve study, Transmission Electron Microscope was used to examine the morphological changes of *Bacillus subtilis* cells before and after overnight treatment with ZnO Nps (MIC X 4). Electron micrographs were taken using a Transmission Electron Microscope (JEM-1400 Plus), the magnification used for the investigated samples was 15000 x.

## Statistical analysis

The data of disc diffusion method were presented as mean ± standard deviation. A Kruskal-Wallis test was performed to determine a significant difference between the mean ranks of at least one pair of groups. Dunn's pairwise tests were carried out for all pairs of groups. All tests were performed using SPSS software. P-values <0.05 were considered statistically significant.

## Results and Discussion

## Characterization of ZnO Nps

## X-ray diffraction (XRD)

The XRD patterns for ZnO Nps, synthesized using co-precipitation and high-speed ball milling methods at different pHs and various ball milling times are shown in Figure 1 (A) and (B), respectively. The XRD spectra revealed the formation of hexagonal ZnO as per JCPDS (card no. 01-79-0206) standards. Figure 1 shows 9 dominant diffraction peaks (100), (002), (101), (102), (110), (103), (200), (112) and (201), which matched with commercially procured ZnO nanopowders (Dutta *et al.,* 2012). The sharpness and intensity of the peaks are quite an indication of the well crystinality nature of the synthesized Nps. No characteristic peaks of impurity phases were observed. The average crystallite sizes were calculated using Scherrer equation and demonstrated in Table 1.

$$D = \frac{K\lambda}{\beta_{hkl} cos\theta}$$

$D$ is the average crystallite size in nanometers, $K$ is a constant equivalent to 0.9, $\lambda$ is the wavelength of the X-ray radiation, $\beta_{hkl}$ is the

peak width at half maximum intensity and $\theta$is the peak position. The calculated average crystalline sizes are inversely proportional to the elevation of pH values and ball milling time. In the co-precipitation method, the average particle size showed a decreasing trend from 100 nm to 41.9 nm as the pH increased from 10 to 13. The possible phenomenon responsible for obtaining smaller crystalline size with the increase in pH values is the supersaturation. Supersaturation is a driving force for crystal nucleation and growth. At high pH values, supersaturation during co-precipitation was higher, promoting nucleation over growth, thus giving smaller particle sizes (Mullin, 2001; Mascolo *et al.,* 2013). The impact of ball milling time on average particle size is also demonstrated, in the current study particles breakage started to occur after 15 minutes of grinding period and maximum particle fracture was observed after 30 minutes of grinding time. Extending time to 45 minutes and 60 minutes caused a very slight mean particle size reduction that seemed to be almost negligible. This finding coincides with other studies that investigated the impact of ball milling time on the mean particle size of ZnO Nps (Kong and Tsuru, 2010; Luo *et al.,* 2017).

## Transmission Electron Microscope (TEM)

TEM images for samples prepared by co-precipitation and high-speed ball milling methods are shown in Figures 2 and 3, respectively. The particle sizes obtained from TEM were in good agreement with the crystalline sizes calculated using XRD technique (Table 1). The nano-structures prepared by co-precipitation method (P1, P2 and P3) had no definite shape, except for P4 that exhibited a needle shaped particle. This finding is consistent with the results obtained by Vaseem *et al.,* (2010) since the reaction was performed out in dry air, the produced ZnO Nps lack defined shape. The absence of definite shape may reveal destructions in recrystallization of ZnO lattice occurred because of high temperature heating process (Look, 2001).

Most ZnO particles that were ball milled for only 15 minutes had a hexagonal shape; however, following ball milling, samples lost their initial hexagonal shape and they were converted into irregular shapes (Mukhtar *et al.,* 2013; Uzun *et al.,* 2016). The obtained irregular particle morphology could be due to energy generated in the milling machine randomly de-agglomerate ZnO particles into smaller fragments with different morphology (Kong and Tsuru, 2010).

## Fourier Transform Infrared Spectroscopy (FTIR)

The FTIR spectra of ZnO Nps prepared by co-precipitation method at different pHs and high-speed ball milling method at diverse ball milling times and illustrated in Figure 4 (A) and (B), respectively were in the range of 4250–250 $cm^{-1}$. The FTIR spectra of the Nps contained number of peaks from 1000 to 4000 $cm^{-1}$ corresponding to carboxylate (COO-) and hydroxyl (O-H) impurities in the materials (Shah *et al.,* 2016).The peak in the region between 433 and 510 $cm^{-1}$belonged to Zn–O (Yuvakkumar *et al.,* 2015). This result indicates the successful production of ZnO Nps. The peaks lying from 1500 to 1700, 2300 to 2700 are representing the functional groups corresponding to C-O symmetric, anti symmetric stretching mode and C-H stretching mode, respectively (Kulkarni and Shirsat, 2015). The absorption tape in the 703-1029 $cm^{-1}$ range represented the lattice vibration of $CO_3^{-2}$ (Wang *et al.,* 2010). The broad band around 3500 $cm^{-1}$ appearing in samples prepared by high-speed ball milling method assigned to O-H stretching mode of hydroxyl group, which represented the presence of water molecule on the surface of ZnO Nps.

The small peaks present in M3 sample between 2830 and 3000 $cm^{-1}$were assigned to C-H stretching vibration of alkane groups (Getie *et al.,* 2017).

## Ultraviolet -Visible Absorption Spectroscopy (UV-vis)

The Ultraviolet- visible absorption spectra of the ZnO Nps prepared by co-precipitation method at different pHs and high-speed ball milling method at different ball milling periods are demonstrated in Figure 5 (A) and (B), respectively. A broad absorption peak was observed in each spectrum at 375-381 nm, no other peaks were observed in the spectrum, which prove the pure synthesis of ZnO Nps. Ultraviolet-Absorption Spectroscopy (UV) analysis showed symmetrical shift in the absorption edge towards the lower wavelength or higher energy region with the decrease in particle size. The blue shift observed in the UV-Vis spectrum with the decline in particles size, was documented in several previous studies (Soosen *et al.,* 2009; Swaroop *et al.,* 2015).

## Antimicrobial activity of ZnO Nps

### Disc diffusion method

The antimicrobial activity for bulk and nano-ZnO suspensions was investigated towards various bacterial and fungal pathogens by disc diffusion method; the results are demonstrated in Table 2. The presence of an inhibition zone clearly proves the antimicrobial effect of ZnO Nps. Interestingly; the size of the inhibition zone varied according to the type of pathogen and ZnO Nps synthesis method. ZnO Nps prepared by co-precipitation method at pH=13 (P4) showed the highest antimicrobial activity followed by ZnO Nps ball milled for 60, 45 and 30 minutes (M4, M3 and M2, respectively), then ZnO Nps prepared by co-precipitation method at pH=12 (P3), afterwards ZnO Nps ball milled for 15 minutes (M1), and finally ZnO Nps prepared by co-precipitation method at pH=11 and pH=10. Amusingly, the size of the inhibition zone increased considerably with decreasing ZnO particle size. Our results proved that the antimicrobial efficiency of ZnO Nps was size-dependent and the antimicrobial activity was inversely proportional to the particle size. These results are consistent with large number of studies that investigated the impact of particle size on the antimicrobial activity of ZnO Nps. ZnO Nps having small size could promote better interactions between their particles and microbial cells (Jeong *et al.,* 2014; da Silva *et al.,* 2019), penetrate easier into bacterial membranes, dissolution of higher concentration of $Zn^{+2}$ (Sirelkhatim *et al.,* 2015), and also generate higher concentration of active oxygen species released from the surface of ZnO (Padmavathy and Vijayaraghavan, 2008).

Regardless of the particle size, the considerable antimicrobial activity of ZnO Np prepared in the current study by co-precipitation method at pH=13 (P4) could be also due to the needle shaped of ZnO Nps. The morphology of the nanostructures can control their mechanism of internalization into the cell wall of bacteria, rods and needles can easily penetrate the cell wall as compared to spherical ZnO Nps (Yang *et al.,* 2009).

In comparison to nanosuspensions, a strong significant difference was noticed between the antimicrobial activity of the bulk and that of the prepared nanoparticles ($p<0.05$). The difference was assessed between bulk ZnO and M2, M3, M4 and P4 ($p<0.05$). There was no evidence of a difference between the bulk ZnO and the other prepared Nps ($p>0.05$). The antimicrobial activity for bulk ZnO was almost negligible. MSRE was the only tested microorganism showing inhibition zone (12 mm) and only growth reduction was noticed

for *Bacillus subtilis.* The reduced effect of bulk ZnO could be due to the fact that most microorganisms have gained resistance against bulk ZnO (Yusof *et al.,* 2019). A study done by Emami-Karvani and Chehourazi (2011) proved that ZnO bulk powder showed no considerable antibacterial activity against *E. coli* and *S. aureus.* Our results are in agreement with other studies that manifested the enhanced antimicrobial efficiency of ZnO Nps as compared to ZnO bulk powder (Padmavathy and Vijayaraghavan, 2008; Tayel *et al.,* 2011).

Among bacterial strains tested, Gram-positive bacteria were more sensitive against ZnO Nps treatment as compared to Gram-negative bacteria. MRSE was the most susceptible Gram-positive bacterium, followed by *Bacillus subtilis*, MRSA, *Bacillus licheniformis* and *Bacillus cereus.* Minimal inhibitory effects were recorded for Gram-negative bacteria; among them, *Enterobacter cloacae* were the most affected followed by *Citrobacter freundii* and *Salmonella* sp.

However; ZnO Nps had no effect against *E. coli* O157:H7. This finding was in conformity with other investigators, who investigated ZnO Nps antimicrobial capability against different bacterial strains belonging to the two groups (Tam *et al.,* 2008; Emami-Karvani and Chehourazi, 2011; Dobrucka *et al.,* 2018). The probable reason behind the variation in ZnO Nps susceptibility against Gram-positive and Gram-negative bacteria is the difference in their cell wall structure (Yu *et al.,* 2004; Tayel *et al.,* 2011; Sirelkhatim *et al.,* 2015).

The antifungal activity of ZnO Nps was investigated against *Penicillium* sp. and *Aspergillus* sp. Our findings were supportive to Gunalan *et al.,* (2012), who stated that ZnO Nps exhibit a promising antifungal activity in addition to their antibacterial effect.

**Minimum inhibitory concentration (MIC) and minimum bactericidal concentration (MBC) of ZnO Nps**

ZnO Nps synthesized by co-precipitation method at pH=13 (P4) was selected to conduct further experiments due to their highest antibacterial effectiveness compared to other prepared Nps. Minimum inhibitory concentration (MIC) and Minimum bactericidal concentration (MBC) were determined for 4 bacteria that were the most susceptible against the prepared Nps. The MIC of ZnONps (as shown in Table 3) recorded for MRSA, MRSE, *Bacillus subtilis* and *Bacillus licheniformis* was found to be 19.53 µg/ml, 9.76 µg/ml, 19.53 µg/ml and 156.25µg/ml, respectively. Concerning the MBC, it was found equivalent to the MIC in the case *Staphylococcus* spp. and *Bacillus subtilis*. However, in case of *Bacillus licheniformis*, the MBC was double the MIC. According to the calculated MIC index, the action of ZnO Nps on the tested pathogens was proved to be bactericidal, and not bacteriostatic. The bacteriocidal action of ZnO Nps was also proved by Xie *et al.,* (2011) and Azam *et al.,* (2012).

**Time kill study**

Three concentrations of ZnO Nps were selected as the antimicrobial treatments in Müller-Hinton broth (MIC X 1, MIC X 2 and MIC X 4). Growth pattern in Müller-Hinton broth lacking ZnO Nps was used as a control for each bacterium under investigation. Ultimate growth characteristics were recognized in control flasks containing medium lacking ZnO Nps. Figure 6 demonstrates the effect of MIC X 1, MIC X 2 and MIC X 4 ZnO Nps on the growth of (A) MRSA (B) MRSE(C) *Bacillus licheniformis* and (D) *Bacillus subtilis*. Monitoring the bacterial growth in culture media supplemented with different concentrations of ZnO Nps clearly showed that the bacterial

growth was almost completely inhibited. All tested concentrations were effective in inhibiting bacterial growth; however, among the three concentrations; MIC X 4 was the most potent antibacterial treatment followed by MIC X 2 then MIC X 1. Thus, these data revealed that the antibacterial activity of ZnO Nps was concentration-dependent. Several previous studies confirmed the concentration–dependent effect of Nps in liquid media (Mirhosseini and Firouzabadi, 2013; 2015).

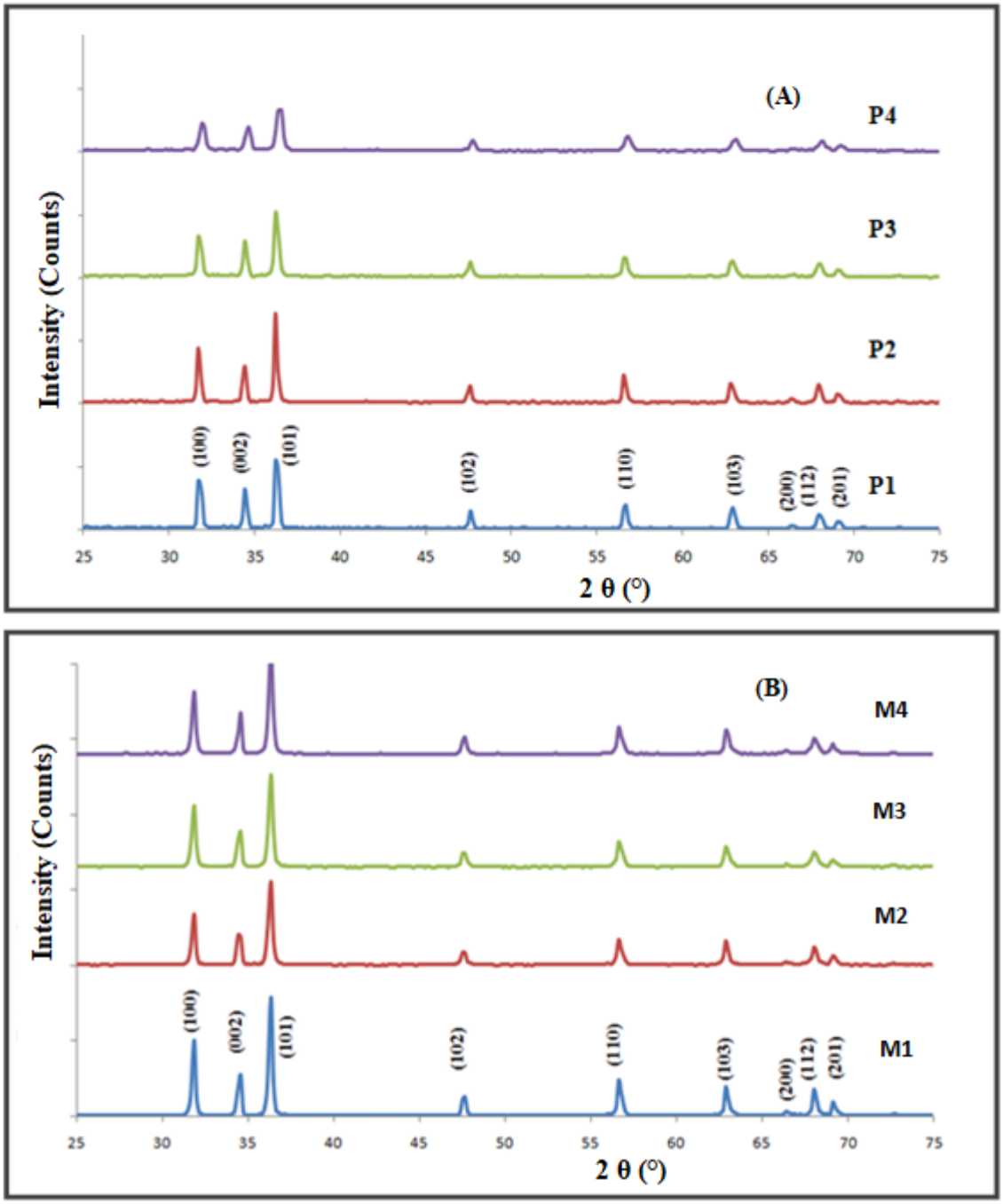


**Figure.1** XRD pattern of ZnO Nps prepared by co-precipitation method at different pH values (A) and high-speed ball milling method at various ball milling time (B)

**Table.1** Average particle size for ZnO Nps prepared by co-precipitation and high-speed ball milling methods

| Characterization Method | Crystalline size (nm) | | | | | | | |
|---|---|---|---|---|---|---|---|---|
| | Co-precipitation method | | | | High-speed ball milling method | | | |
| | P1 | P2 | P3 | P4 | M1 | M2 | M3 | M4 |
| XRD | 100.0 | 92.5 | 61.8 | 41.9 | 70.1 | 53.7 | 53.6 | 52.0 |
| TEM | 101.0 | 93.6 | 62.8 | 43.0 | 73.0 | 58.3 | 58.0 | 56.0 |

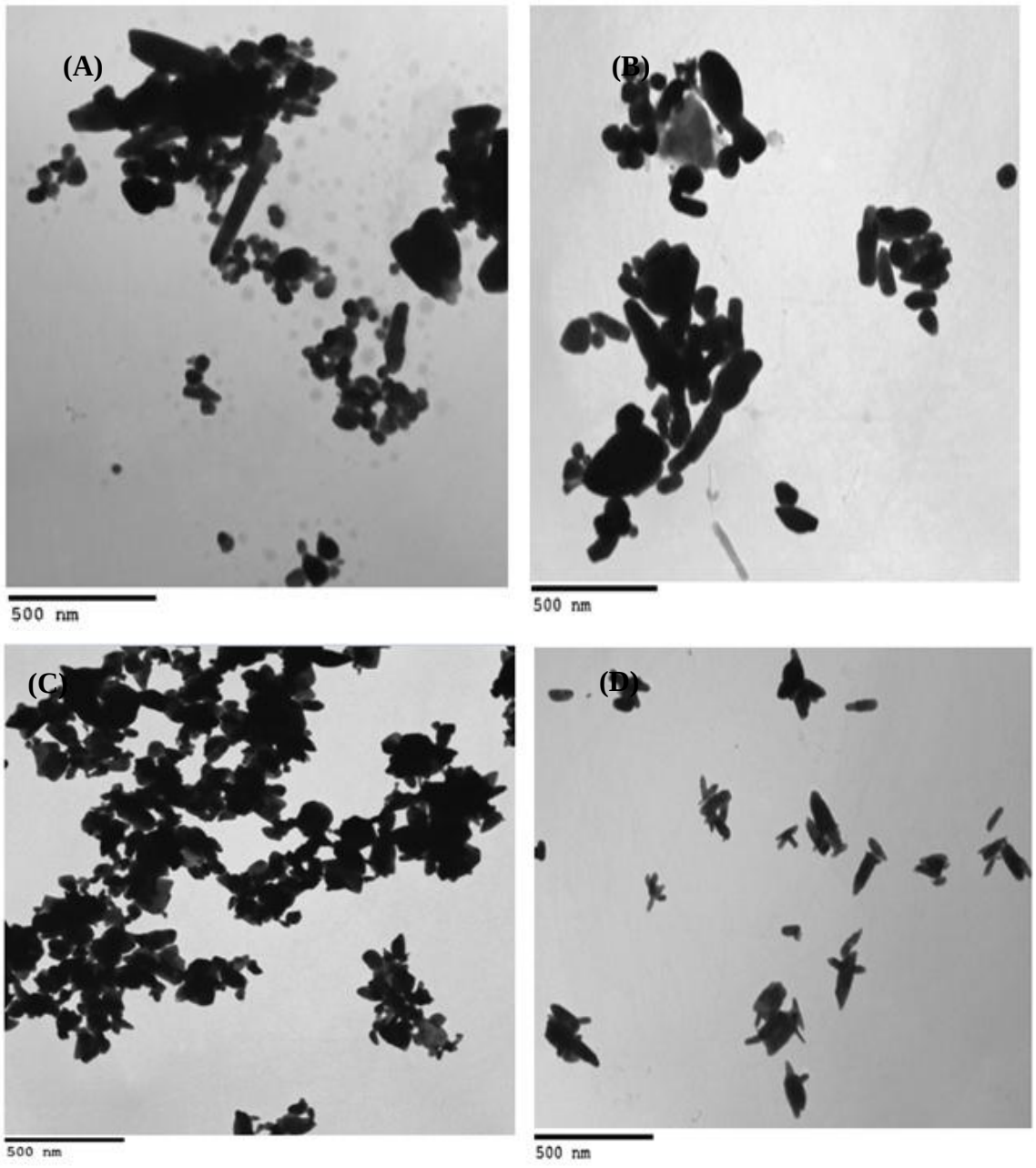


**Figure.2** Transmission Electron Microscope images for ZnO Nps prepared by precipitation method, at P1 (A), P2 (B), P3 (C) and P4 (D).

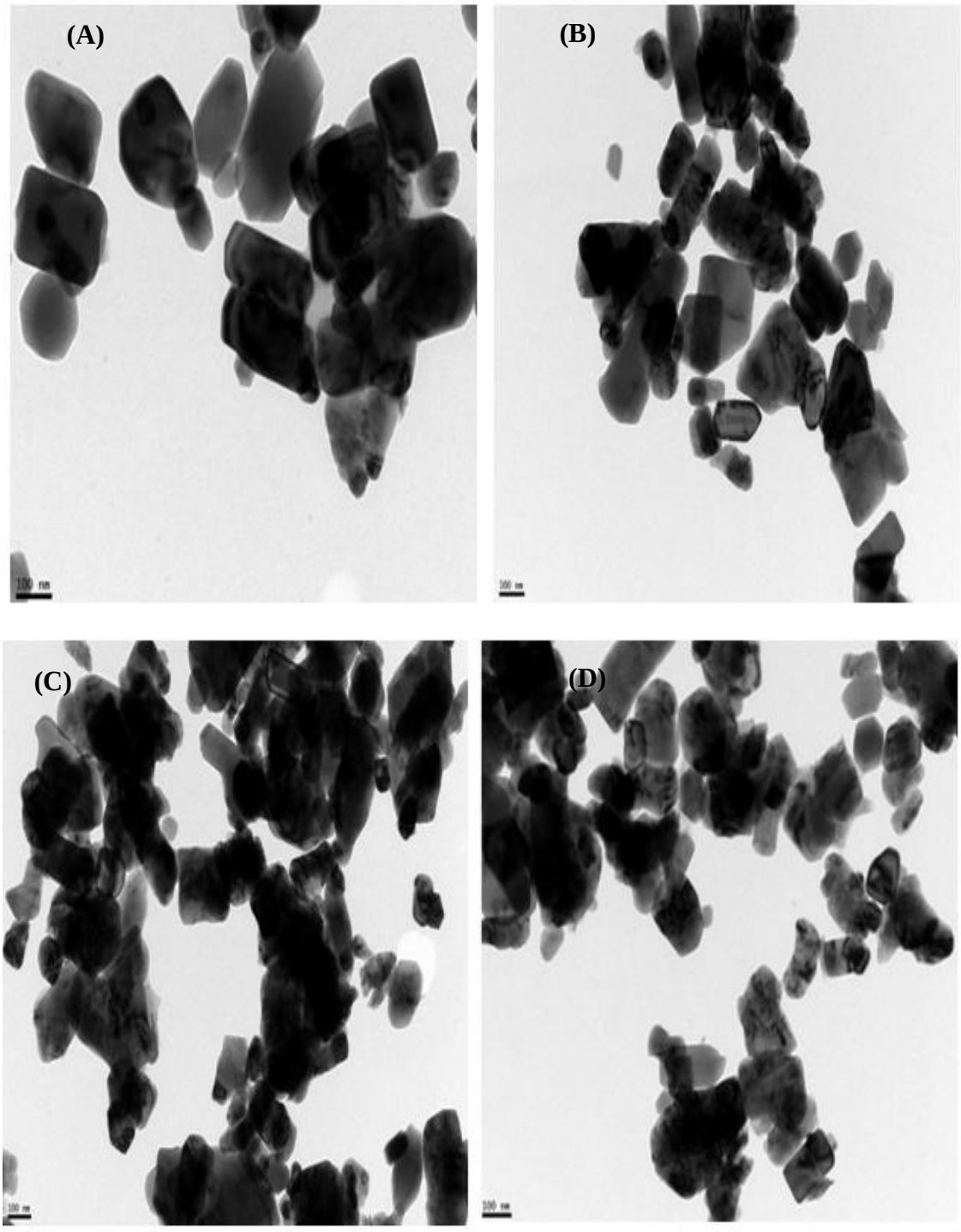


**Figure.3** Transmission Electron Microscope images for ZnO Nps prepared by high-speed ball milling method, M1 (A), M2 (B), M3 (C) and M4 (D)

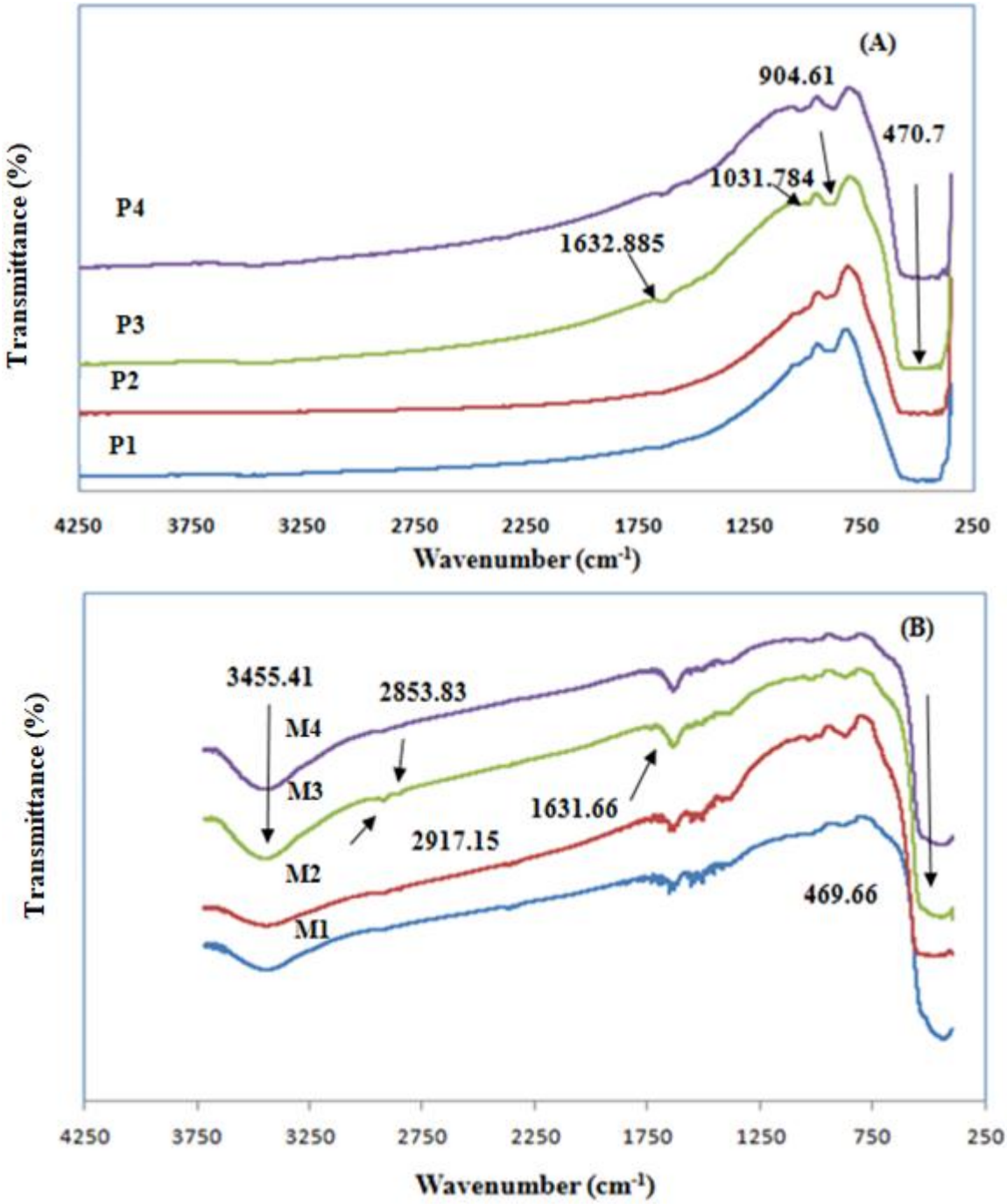


**Figure.4** FTIR for ZnO Nps prepared by co-precipitation method under different pH values (A) and high-speed ball milling method with various ball milling times (B).

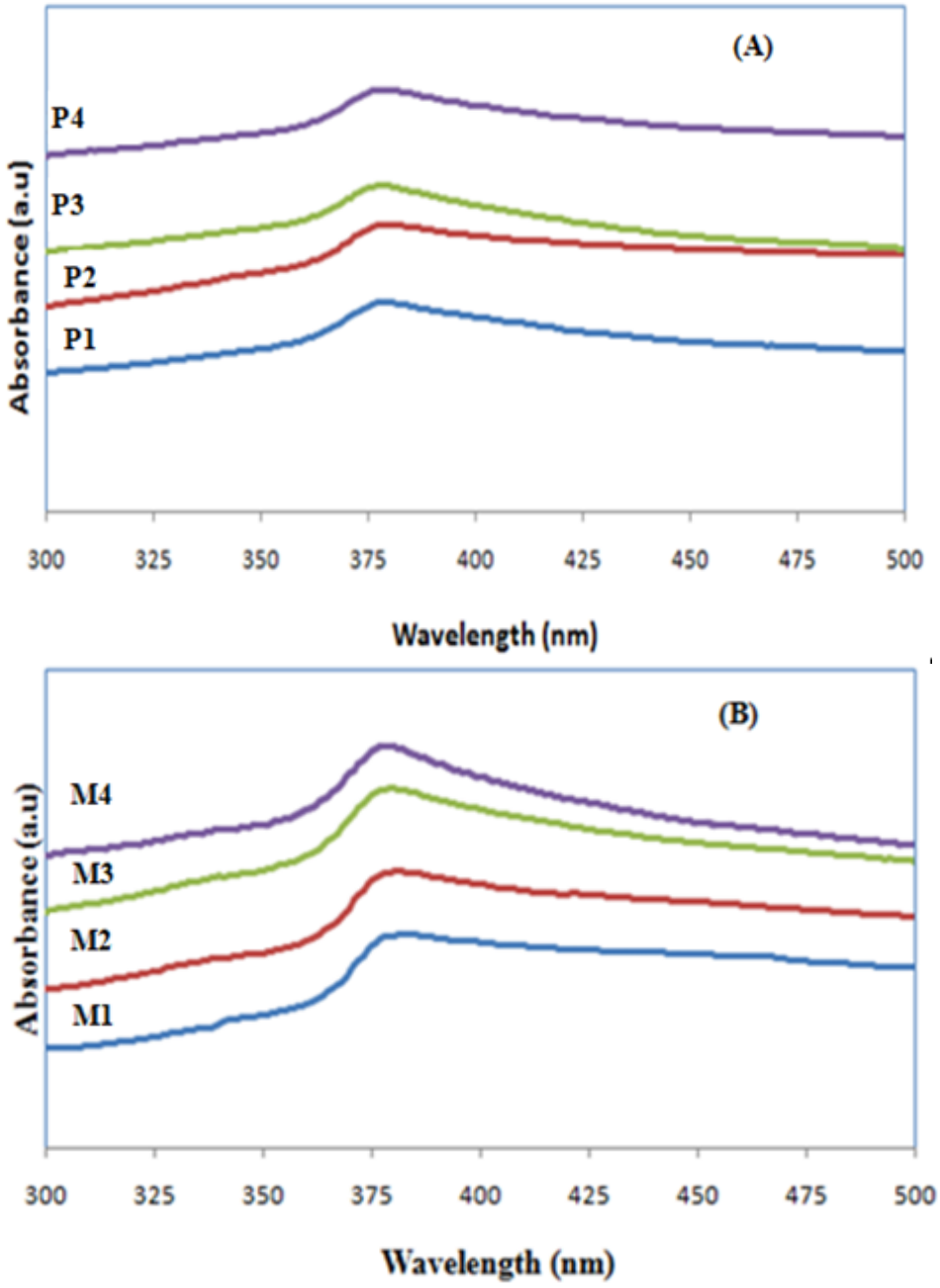


**Figure.5** UV-visible absorption spectra for ZnO Nps prepared by co-precipitation Method under different pH values (A) and high-speed ball milling method with various ball milling times (B).

**Table.2** Mean diameters of inhibition zones recorded for microorganisms treated with bulk and ZnO Nps prepared by co-precipitation and high-speed ball milling methods.

| Mean diameters of inhibition zones (mm) | | | | | | | | | | |
|---|---|---|---|---|---|---|---|---|---|---|
| **Microorganism** | Co-precipitation method (pH) | | | | Ball milling method Time (minutes) | | | | Bulk ZnO | Positive control |
| | P1 | P2 | P3 | P4 | M1 | M2 | M3 | M4 | | |
| **MRSA** | 11.5 | 12 | 16 | 22 | 14 | 17 | 17 | 17.5 | --- | 15 |
| **MRSE** | 16 | 17 | 21 | 27 | 19 | 24 | 24 | 24.5 | 12 | 17 |
| ***Bacillus cereus*** | --- | --- | 12 | 16 | 10 | 13 | 13 | 13 | --- | 29 |
| ***Bacillus subtilis*** | 14 | 14 | 17 | 25 | 16 | 21 | 21 | 21 | Gr | 31 |
| ***Bacillus licheniformis*** | 10 | 10 | 14 | 19 | 12 | 15 | 15 | 15 | --- | 31 |
| ***Enterobacter cloacae*** | --- | --- | --- | 13 | --- | 11 | 11 | 11 | ---- | 28 |
| ***Salmonella* sp.** | --- | --- | --- | 11 | --- | 9 | 9 | 9 | --- | 30 |
| ***Ecoli*O157:H7** | --- | --- | --- | --- | --- | --- | --- | --- | --- | 30 |
| ***Citrobacterfreundii*** | --- | --- | --- | 12.5 | --- | 10 | 10 | 10 | --- | 23 |
| ***Aspergillus* sp.** | 10 | 10 | 14 | 18 | 12 | 15 | 15 | 15 | --- | 26 |
| ***Penicilliumsp.*** | --- | --- | 11 | 15 | 10 | 13 | 13 | 13 | --- | 33 |

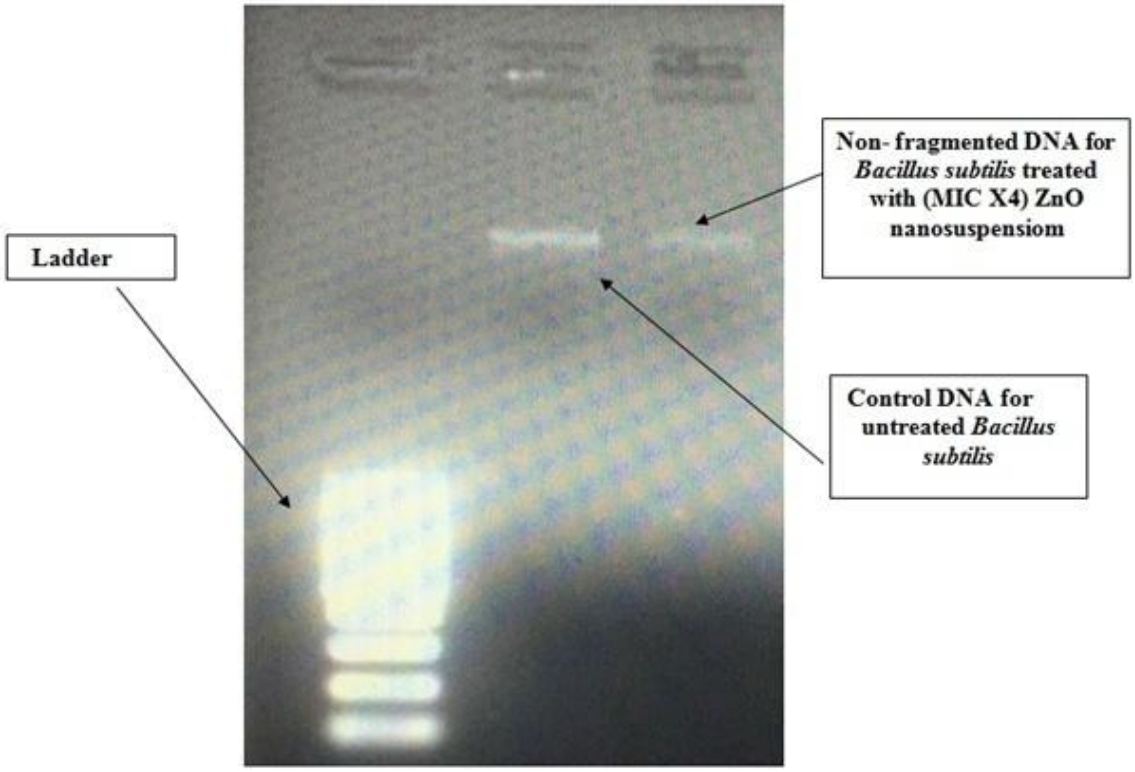


**Figure.8** Gel Electrophoresis for DNA of *Bacillus subtilis*, untreated and treated with ZnO nanosuspension

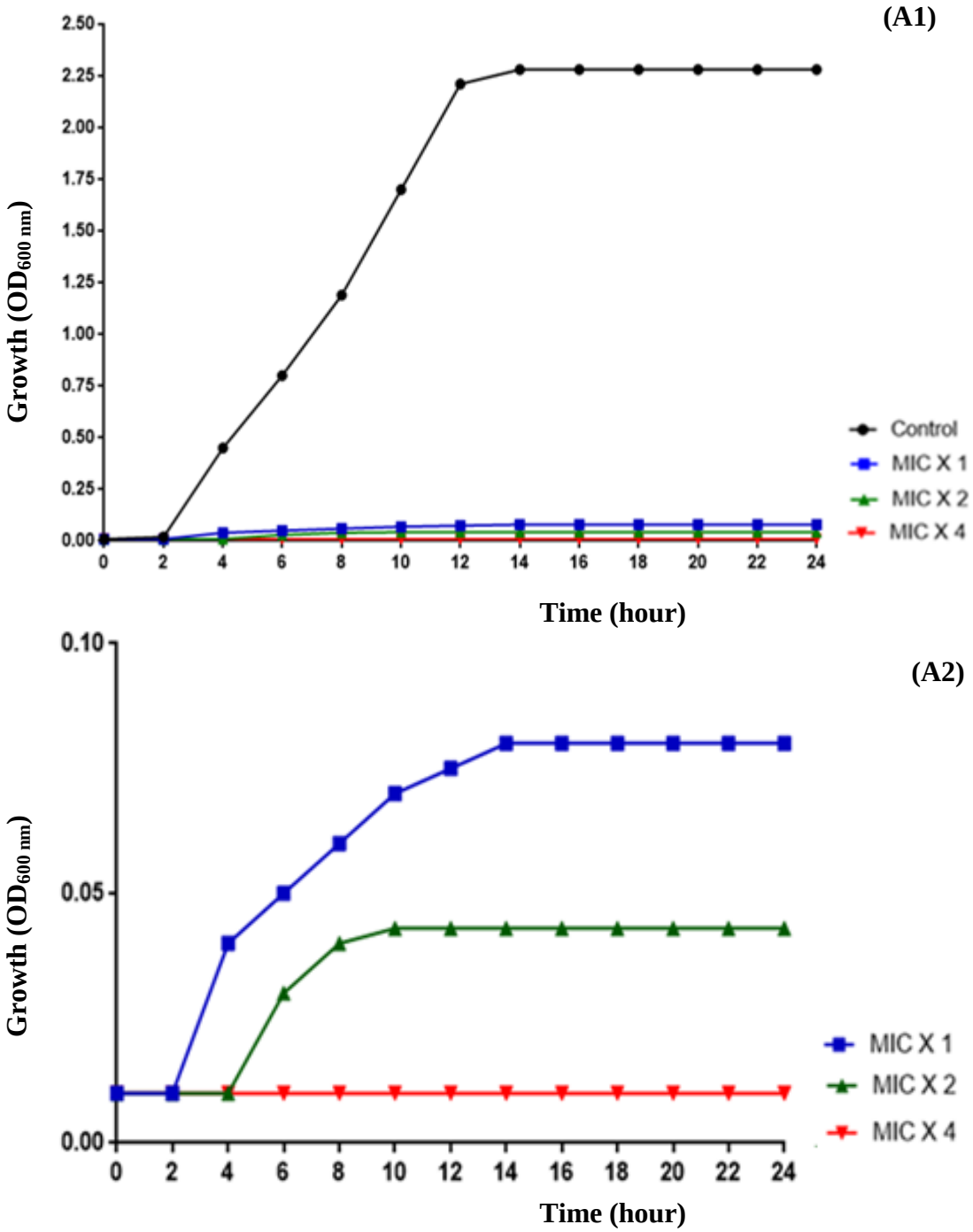


**Figure.6** Effect of MIC X 1, MIC X 2 and MIC X 4 of ZnO Nps synthesized by co-precipitation method at pH=13 (P4)on the growth of MRSA(A1 & A2), MRSE(B1 & B2), *Bacillus licheniformis* (C1 & C2)and *Bacillus subtilis*D1 & D2) in the MHB at 37 ºC during different time intervals.

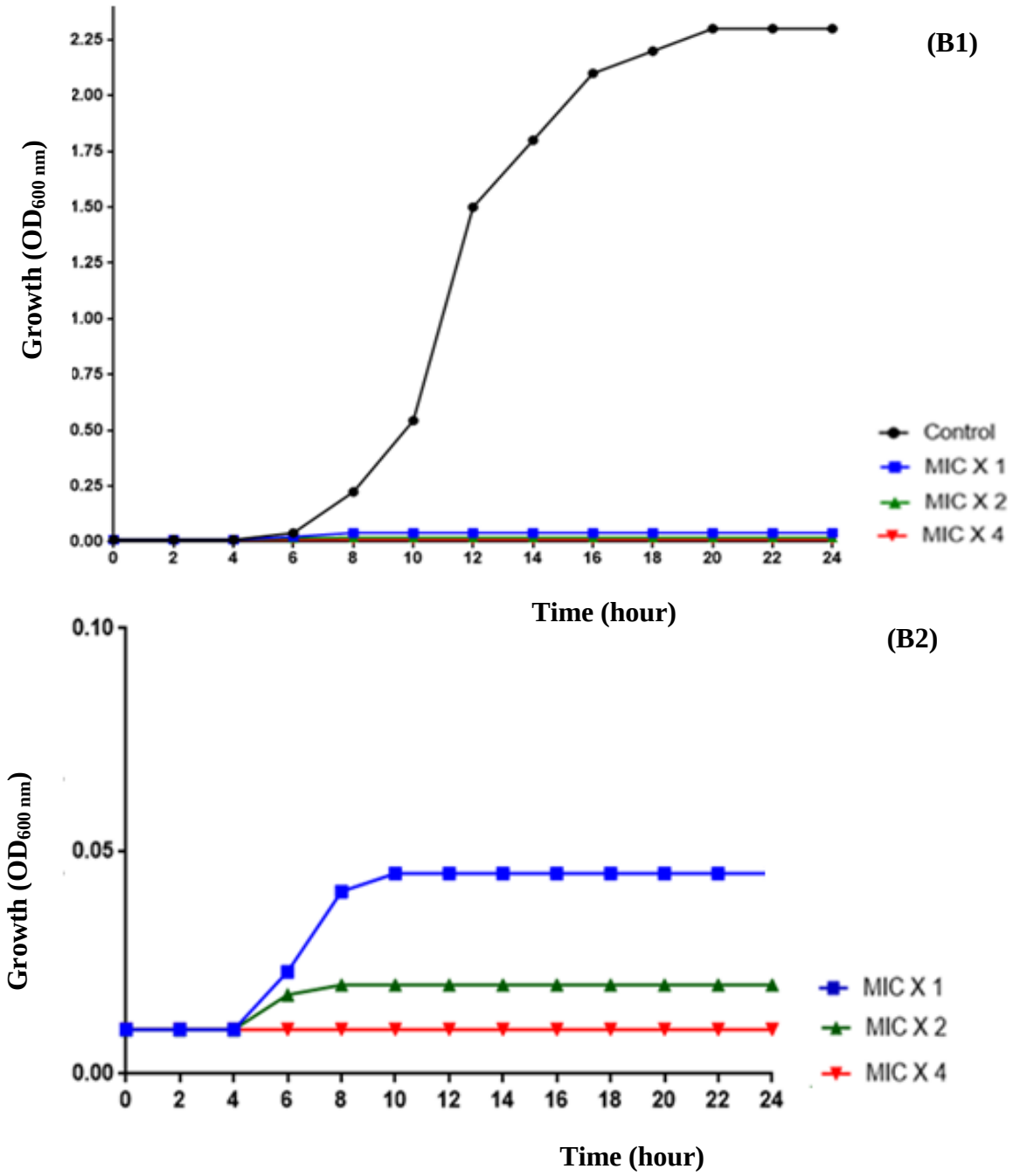


**Figure 6: Continued**

**(C1)**

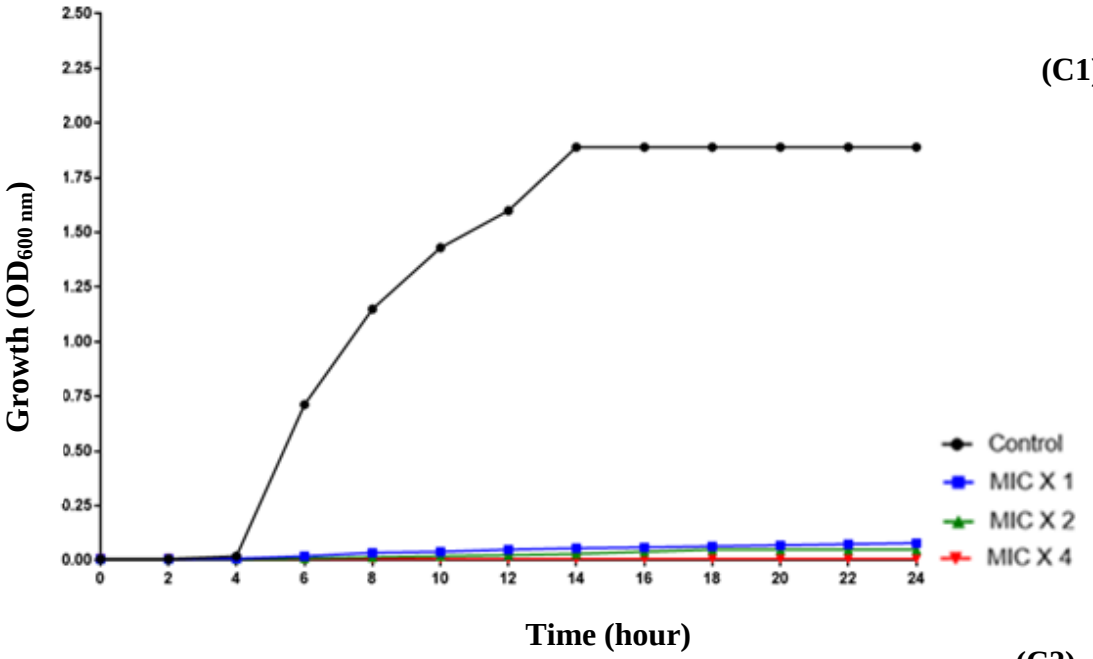


**(C2)**

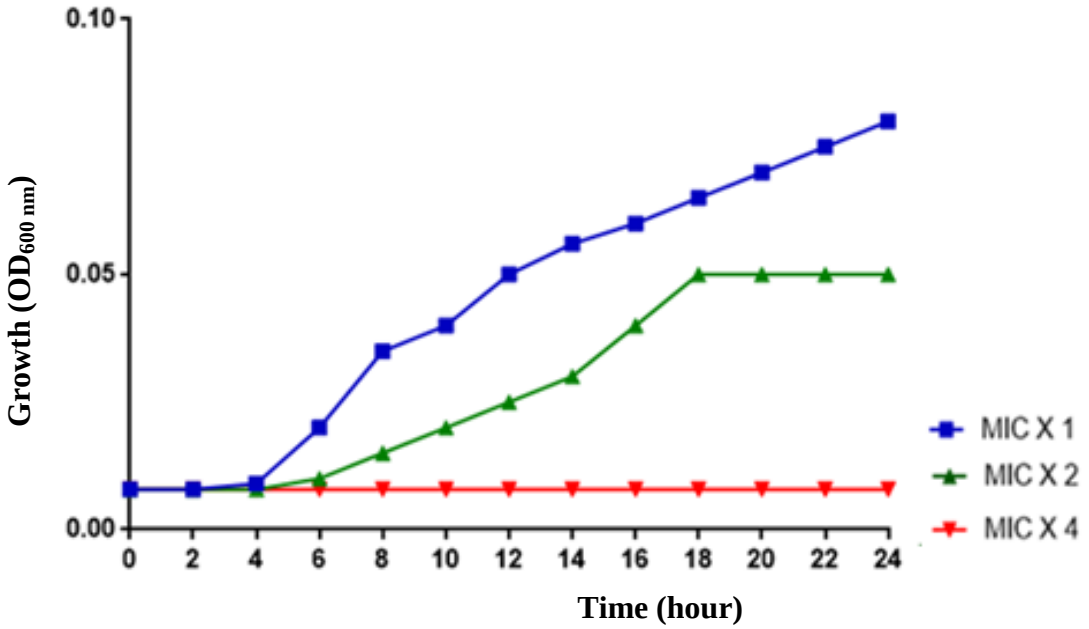


**Figure 6: Continued**

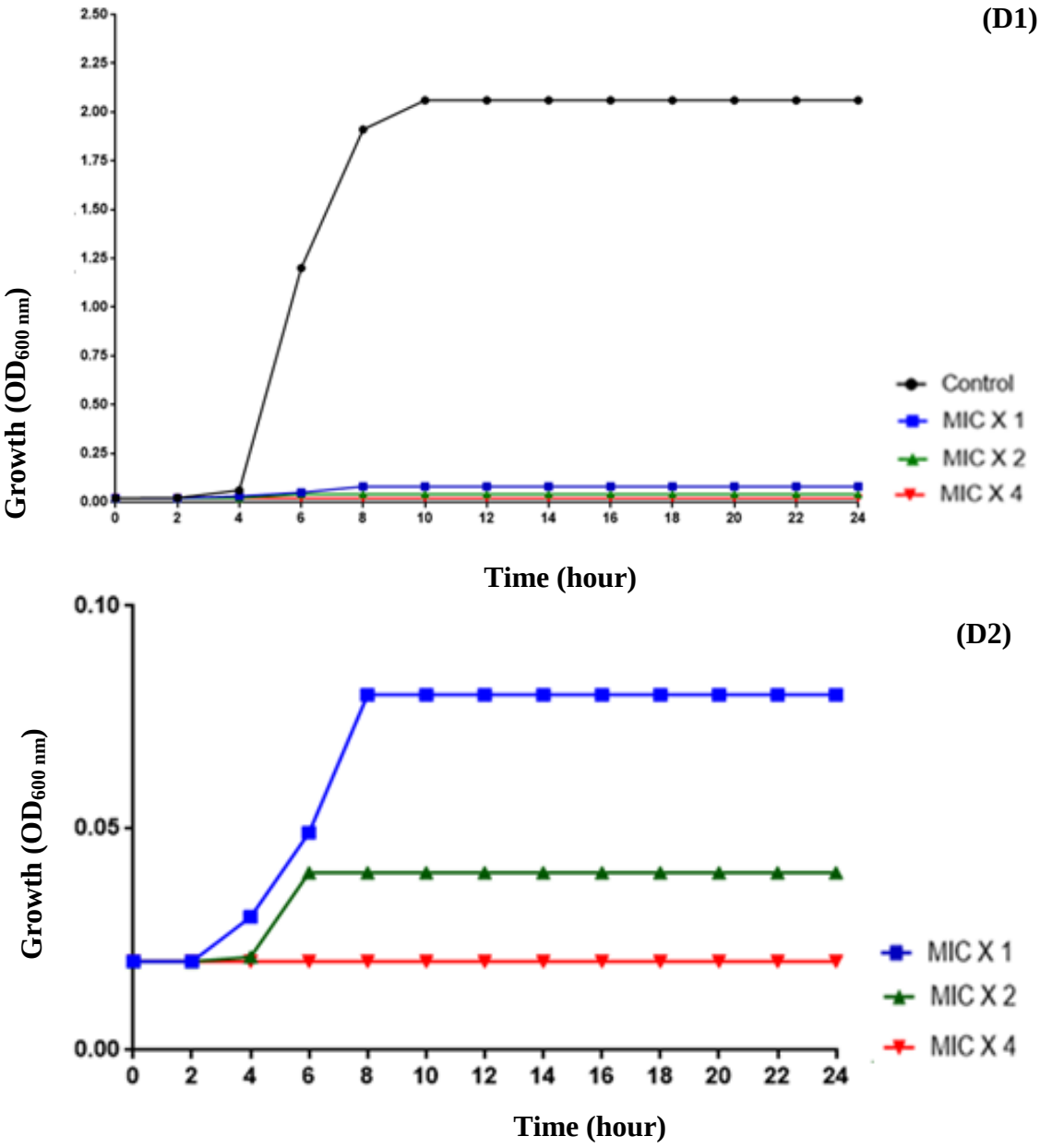


**Figure 6: Continued**

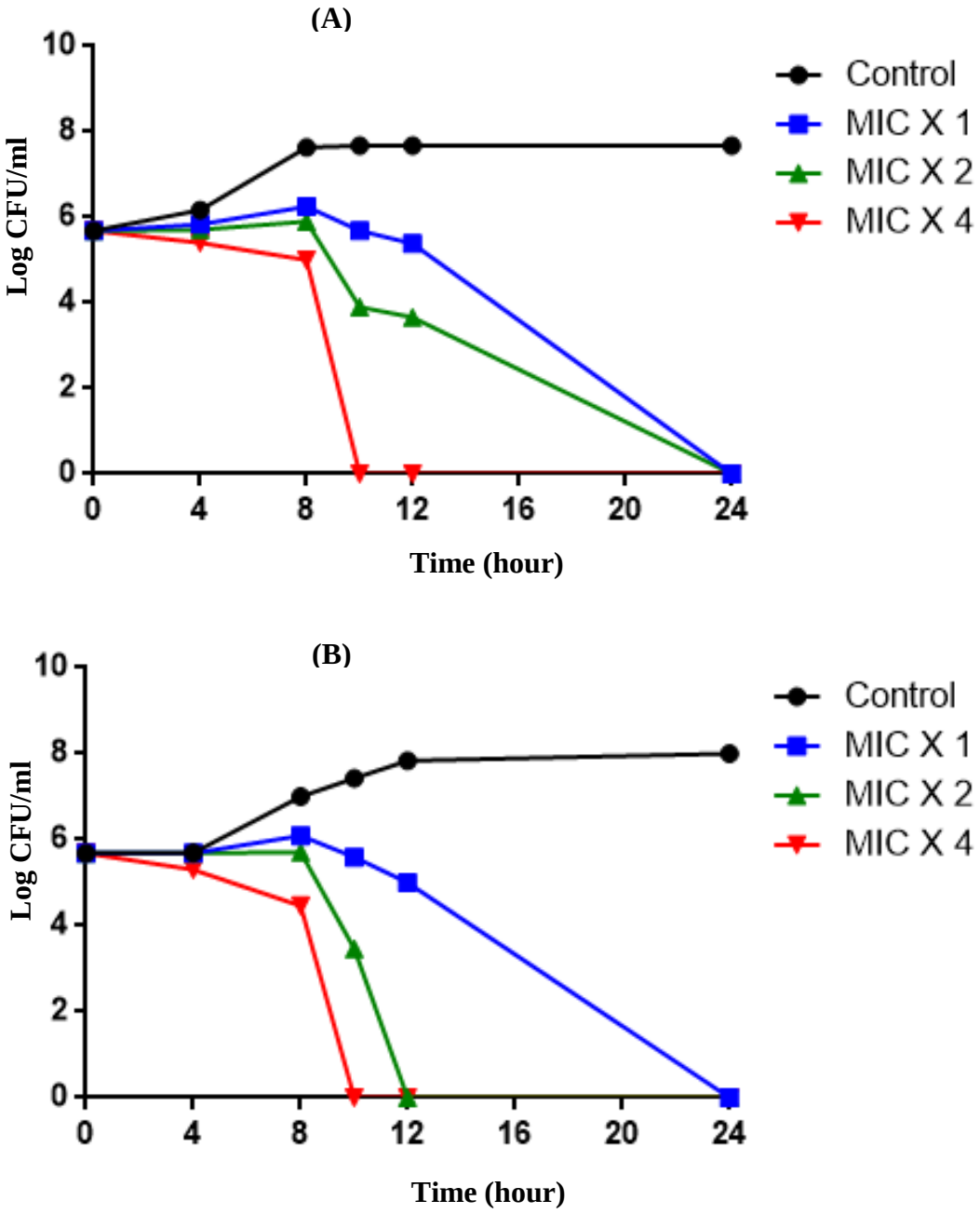


**Figure.7** The effect of MIC X 1, MIC X 2 and MIC X 4 ZnONps synthesized by co-precipitation method at pH=13 (P4)on the growth of *Bacillus subtilis* (A) and MRSE (B) in sterile Candia milk during different time intervals.

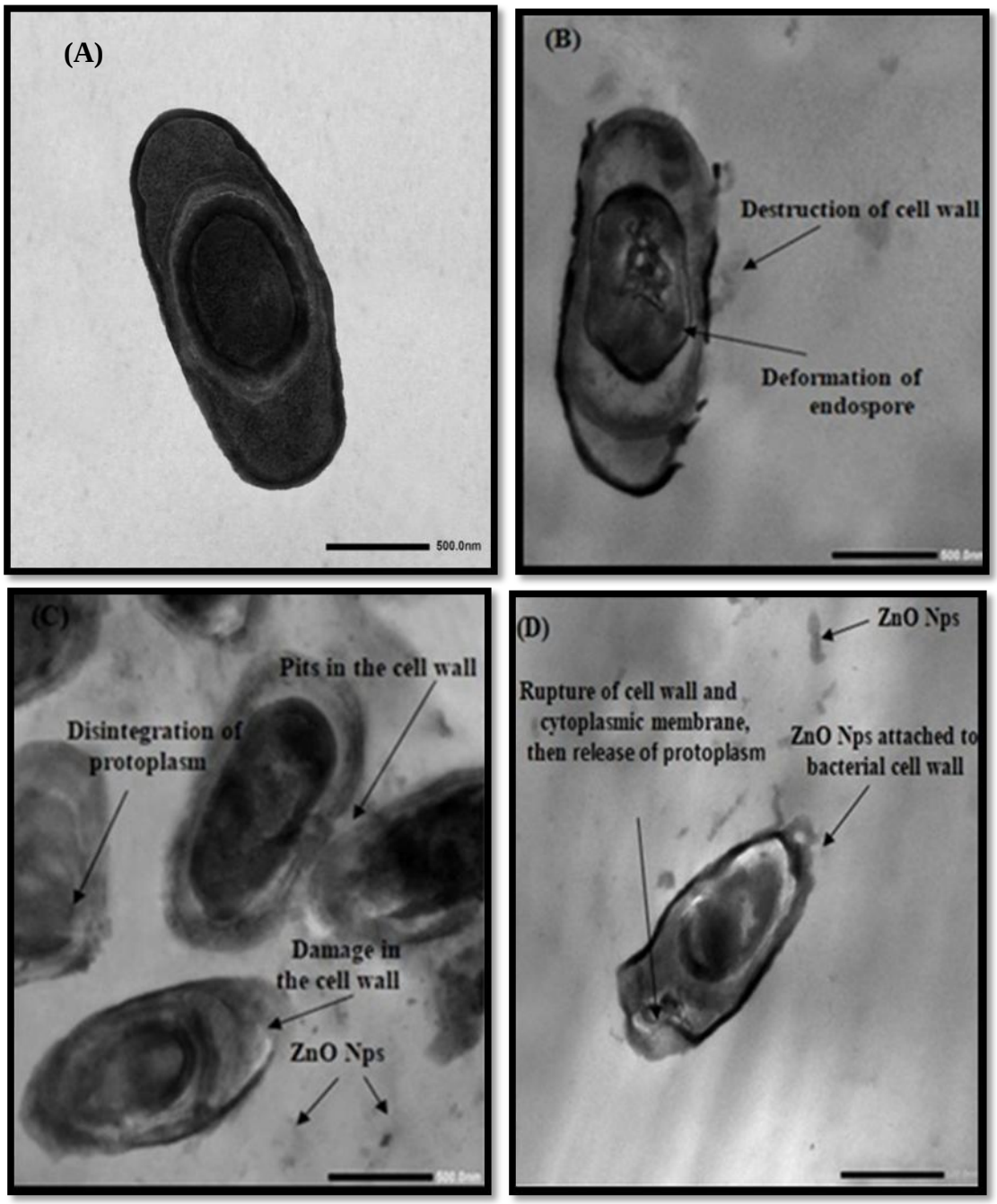


**Figure.9** TEM images for *Bacillus subtilis*, untreated (A) and treated with nanosuspensions (B, C and D).

**Table.3** Minimum inhibitory (MIC) and minimum bactericidal (MBC) concentrations of ZnO Nps synthesized by co-precipitation method at pH=13 (P4) and tested against some bacteria.

| Bacterium | MIC (µg/ml) | MBC (µg/ml) | MIC index (MBC/MIC) |
|---|---|---|---|
| **MRSA** | 19.53 | 19.53 | <4 |
| **MRSE** | 9.76 | 9.76 | <4 |
| ***Bacillus subtilis*** | 19.53 | 19.53 | <4 |
| ***Bacillus licheniformis*** | 156.25 | 312.50 | <4 |

## Application of ZnO Nps in milk samples

Milk is exceedingly susceptible to spoilage by microorganisms (Gunasekera *et al.*, 2002). In sterile milk samples inoculated with *Bacillus subtilis* and MRSE(The most susceptible tested microorganisms),three concentrations of ZnO Nps (MIC X 1, MIC X 2 and MIC X 4) were introduced as antimicrobial agents. A sterile milk sample was used as a negative control. Treatments with various concentrations of ZnO Nps had a significant lethal effect on MRSE as well as on *Bacillus subtilis* during 24 hours of incubation, compared to the control (Figure 7). MIC X 4 was the most effective compared to other ZnO Nps concentrations tested against both bacterial strains. After 24 hours of incubation, complete growth disappearance was observed for *Bacillus* and *Staphylococcus* cells treated with all tested concentrations of ZnO Nps.

The finding of the current study revealed that ZnO Nps exhibits a preferential ability to suppress and reduce *Bacillus subtilis* and MRSE cells in milk. Emamifar *et al.*, (2011) also investigated the antimicrobial activity of ZnO Nps in orange juice inoculated with 8.5 log CFU/ml of *Lactobacillus plantarum*. The results proved that ZnO Nps remarkably reduced the rate of microbial growth. Mirhosseini and Firouzabadi (2013) investigated the efficiency of ZnO Nps against *E. coli* and *S. aureus* in milk samples, the study suggested that ZnO Nps could be effective antibacterial agent in food preservation. ZnO Nps were used for controlling *Listeria monocytogenes* and *Bacillus cereus* contaminations in milk samples collected in Iran, the study proved that ZnO nanostructures had the potential for being applied in food systems to prolong the durability of milk (Mirhosseini and Firouzabadi, 2015).

## Gel Electrophoresis for DNA of *Bacillus subtilis* treated with ZnO Nps

The effect of ZnO Nps on bacterial DNA was assessed by gel electrophoresis. *Bacillus subtilis* was the chosen bacterial strain for the study since *Bacillus* spp. were noted by many researches as the most widespread foodborne pathogen (Zhou *et al.*, 2008; Bang *et al.*, 2017). The MIC X4 of ZnO Nps, which showed the most compelling effect, was used as a selected concentration. No degradation in the DNA of *B. subtilis* cells treated with ZnO Nps was observed. However, thicker DNA band of untreated cells compared to the DNA of treated cells, was noticed although same volumes were loaded on the gel, which could be due to the inhibition of bacterial growth leading to lowering DNA yield (Figure 8). This result was in conformity with Ghasemi and Jalal (2016), who proved that no bacterial

DNA fragmentation was observed after ZnO nano-treatment.

### Transmission Electron Microscope (TEM)

TEM microscopy was performed to visualize the morphological changes in cells of *Bacillus subtilis* upon exposure to ZnO Nps. The shape, the cell wall and the intracellular structures of untreated cells were intact (Figure 9A). On the contrary, the micrographs clearly illustrate that the treated *Bacillus* cells with ZnO Nps were damaged, disintegration of cell wall, cytoplasmic membrane and protoplasm were noticed (Figure 9B, C and D). Leakage of protoplasm was also remarked in Figure 9(D). These observations were reported by many investigators (Liu *et al.*, 2009; Padmavathy and Vijayaraghavan, 2011) and suggest that ZnO Nps interact with biomolecules causing cell apoptosis leading to cell death (Siddiquah *et al.*, 2018). Moreover, the probable suggestion for the membrane damage is the electrostatic interaction between ZnO Nps and cell surfaces causing cellular internalization of ZnO Nps (Stoimenov *et al.*, 2002; Fu *et al.*, 2005; Márquez *et al.*, 2018).

Recently, the need for novel technologies to control foodborne pathogens is increasing, due to the alarming increase in fatalities and hospitalization worldwide. The current study revealed the sensitivity of some foodborne pathogens against ZnO Nps. Based on our findings, ZnO Np can be recommended as antimicrobial agents which may be incorporated in active food packaging but, after confirming their biosafety. Future research is required for low-cost preparation of ZnO Nps having smallest particle sizes of high purity.

## References

Aamer, A.A., Abdul-Hafeez, M.M., and Sayed, S.M. 2014. Minimum inhibitory and bactericidal concentrations (MIC and MBC) of honey and bee propolis against multi-drug resistant (MDR) *Staphylococcus* sp. isolated from bovine clinical mastitis. Alternative and Integrative Medicine, 3, https://doi.org/10.4172/2327-5162.1000171.

Ahamed, J.A., and Kumar, V.P. 2016. Synthesis and characterization of ZnO nanoparticles by co-precipitation method at room temperature. Journal of Chemical and Pharmaceutical Research, 8: 624-628.

Arciniegas-Grijalba, P.A., Patin˜o-Portela, M.C., Mosquera-Sa´nchez, M.C., Guerrero-Vargas, J.A., and Rodrı´guez-Pa´ez, J.E. 2017. ZnO nanoparticles (ZnO-NPs) and their antifungal activity against coffee fungus *Erythricium salmonicolor*. Applied Nanoscience, 7: 225-241.

Azam, A., Ahmed, S. A., Oves, M., Khan, S.M., Habib, S.S., and Memic, A. 2012. Antimicrobial activity of metal oxide nanoparticles against Gram-positive and Gram-negative bacteria: a comparative study. International Journal of Nanomedicine, 7: 6003-6009.

Azeredo, D. H. 2013. Antimicrobial nanostructures in food packaging. Trends Food Science and Technology, 30: 56–69.

Bang, M.S., Jeong, H.W., Lee, Y.J., Oh, H.Y., Lee, S.J., Shim, M.S., Shin, J.I., and Oh, C.H. 2017. Draft genome sequences of *Bacillus subtilis* strain DKU_NT_01 isolated from traditional Korean food containing soybean (chung-gook-jang). Genome Announcements, 5: doi: 10.1128/genomeA.00769-17.

Beyth, N., Houri-Haddad, Y., Domb, A., Khan, W., and Hazan, R. 2015. Alternative antimicrobial approach: nano-antimicrobial materials. Evidence-Based Complementary and Alternative Medicine, 2015: 1-16.

Bhattacharyya, P., Agarwal, B., Goswami, M., Maiti, D., Baruah, S., and Tribedi, P. 2018. Zinc oxide nanoparticle inhibits the biofilm formation of *Streptococcus pneumoniae*. Antonie Van Leeuwenhoek, 111: 89- 99.

Brayner, R., Ferrari-Iliou, R., Brivois, N., Djediat, S., Benedetti, M., and Fievet, F. 2006. Toxicological impact studies based on *Escherichia coli* bacteria in ultrafine ZnO nanoparticles colloidal medium. Nano Letters, 6: 866–870.

Buzea, C., Pacheco, I.I., and Robbie, K. 2007. Nanomaterials and nanoparticles: Sources and toxicity. Biointerphases, 2: MR17, https://doi.org/10.1116/1.2815690.

Clinical and Laboratory Standard Institution (CLSI) 1999. CLSI document M26-A. Methods for determining bactericidal activity of antimicrobial agents; approved standard -Volume 19 No: 18. Wayne, Pennsylvania, USA: Clinical and Laboratory Standards Institute.

Clinical and Laboratory Standard Institution (CLSI) 2010. CLSI document M51-A. Reference method for antifungal disk diffusion susceptibility testing of non-dermatophyte filamentous fungi; approved guideline. Wayne, Pennsylvania, USA: Clinical and Laboratory Standards Institution.

Clinical and Laboratory Standard Institution (CLSI) 2012. CLSI document M02-A11. Performance standards for antimicrobial disk susceptibility tests; approved standard-eleventh Edition. Wayne, Pennsylvania, USA: Clinical and Laboratory Standards Institute.

Clinical and Laboratory Standard Institution (CLSI) 2012. CLSI document M07-A9. Methods for dilutions antimicrobial susceptibility tests for bacteria that grow aerobically; approved standards–ninth Edition. Wayne, Pennsylvania, USA: Clinical and Laboratory Standards Institution.

da Silvaa, B.L., Caetanoa, B.L., Chiari-Andreoa, B.G., Pietroa, R.C.L.R., and Chiavaccia, L.A. 2019. Increased antibacterial activity of ZnO nanoparticles: Influence of size and surface modification. Colloids and Surfaces B: Biointerfaces, 177: 440-447.

Díez-Pascual, A.M. 2018. Antibacterial activity of nanomaterials. Nanomaterials, 8: 359-364.

Dobrucka, R., and Dugaszewska, J. 2016. Biosynthesis and antibacterial activity of ZnO nanoparticles using *Trifolium pratense* flower extract. Saudi Journal of Biological Sciences, 23: 517-523.

Dutta, R.K., Nenavathu, B.P., Gangishetty, M.K., and Reddy, A.V.R. 2012. Studies on antibacterial activity of ZnO NPs by ROS induced lipid peroxidation. Colloid and Surfaces B: Biointerfaces, 94: 143–150.

Emami-Karvani, Z., and Chehrazi, P. 2011. Antibacterial activity of ZnO nanoparticle on Gram-positive and Gram-negative bacteria. African Journal of Microbiology Research, 5: 1368-1373.

Fu, G., Vary, P. S., and Lin, C. T. 2005. Anatase TiO2 nanocomposites for antimicrobial coatings. Journal of Physical Chemistry B, 109: 8889-8898.

Getie, S., Belay, A., Chandra, Reddy, A.R., and Belay, Z. 2017. Synthesis and characterizations of zinc oxide nanoparticles for antibacterial applications. Journal of Nanomedicine and Nanotechnology, 8: doi: 10.4172/2157-7439.S8-004.

Ghasemi, F., and Jalal, R. 2016. Antimicrobial action of zinc oxide nanoparticles in combination with ciprofloxacin and ceftazidime against multidrug-resistant Acinetobacter baumannii. Journal of Global Antimicrobial Resistance, 6: 118-122.

Gunalan, S., Sivaraj, R., and Rajendran, V. 2012. Green synthesized ZnO nanoparticles against bacterial and fungal pathogens. Progress in Natural Science: Material International, 22: 693-700.

Gunasekera, T.S., Sorensen, A., Attfield, P.V., Sorensen, J., and Veal, D.A. 2002. Inducible gene expression by non-culturable bacteria in milk after pasteurization. Applied and Environmental Microbiology, 68: 1988-1993.

Jalal, R., Goharshadi, E.K., Abareshi, M., Moosavi, M., Yousefi, A., and Nancarrow, P. 2010. ZnO nanofluids: green synthesis, characterization, and antibacterial activity. Materials Chemistry and Physics, 121: 198–201.

Jasim, N.O. 2015. Antifungal activity of zinc oxide nanoparticles on *Aspergillus fumigatus* fungus and *Candida albicans* yeast. Journal of Natural Sciences Research, 5: 23-27.

Jeong, Y., Lim, D.W., and Choi, J. 2014. Assessment of size-dependent antimicrobial and cytotoxic properties of silver nanoparticles. Advances in Materials Science and Engineering, 2014: 1-9.

Jones, N., Ray, B., Ranjit, K.T., and Manna, A.C. 2008. Antibacterial activity of ZnO nanoparticle suspensions on a broad

spectrum of microorganisms. FEMS Microbiology Letters, 279: 71-76.

Khan, S.T., Ahamed, M., Musarrat, J., and Al-Khedhairy, A.A. 2014. Anti-biofilm and antibacterial activities of zinc oxide nanoparticles against the oral opportunistic pathogens *Rothia dentocariosa* and *Rothia mucilaginosa*. European Journal of Oral Sciences, 122: 397-403.

Kone, W.M., Kamanzi, A.K., Terreaux, C., Hostettmann, K., Traore, D., and Dosso, M. 2004. Traditional medicine in North Côte-d'Ivoire: screening of medicinal plants for antibacterial activity. Journal of Ethnopharmacology, 93: 43-49.

Kong, C., and Tsuru, T. 2010. Zeolite nanocrystas prepared from zeolite microparticles by a centrifugation – assisted grinding method. Chemical Engineering and Processing, 49: 809-814.

Kulkarni, S.S., Shirsat, M.D. 2015. Optical and structural properties of zinc oxide nanoparticles. International Journal of Advanced Research in Physical Science, 2: 14-18.

Liu, Y., He, L., Mustapha, A., Li, H., Hu, Q. Z., and Lin, M. 2009. Antibacterial activities of zinc oxide nanoparticles against *Escherichia coli* O157:H7. Journal of Applied Microbiology, 107:

Look, D.C. 2001. Recent advance in ZnO materials and devices. Materials Science and Engineering, 80: 378-383.

Luo, Y., Ran, G., Chen, N., and Wang, C. 2017. Microstructure and morphology of Mo-based Tm2O3 composites synthesized by ball milling and sintering. Advanced Powder Technology, 28: 658-664.

Madigan, M., Mertinko, J., and Brock, T. 2006. Brock biology of microorganisms. Pearson Prentice Hall, USA.

Manna, A.C. 2012. Synthesis, characterization, and antimicrobial activity of zinc oxide nanoparticles. In: Cioffi N, Rai M (Eds.). Nano-antimicrobials: Progress and prospects. Berlin, Germany: Springer-Verlag Berlin Heidelberg, pp. 151-180.

Márquez , I.G., Ghiyasvand, M., Massarsky, A., Babu, M., Samanfar, B., Omidi, K., Thomas, W., Moon, T.W., Smith , M.L., and Golshani, A. 2018. Zinc oxide and silver nanoparticles toxicity in the baker's yeast, *Saccharomyces cerevisiae*. PLOS ONE, 13: e0193111. https://doi.org/10.1371/journal.pone.0193111.

Mascolo, C.M., Pei, Y., and Ring, A.T. 2013. Room temperature co-precipitation synthesis of magnetite nanoparticles in large pH window with different bases. Materials, 6: 5549-5567.

Mirhosseini, M., and Firouzabad, B. F. 2013. Antibacterial activity of zinc oxide nanoparticle suspensions on food-borne pathogens. International Journal of Dairy Technology, 66: 291-295.

Mirhosseini, M., and Firouzabad, B.F. 2015. Reduction of *Listeria monocytogenes* and *Bacillus cereus* in milk by zinc oxide nanoparticles. Iranian Journal of Pathology, 10: 97-104.

Mukhtar, N.Z.F., Borhan, M.Z., Rusop, M., and Abdullah, S. 2013. Effect of milling time on particle size and surface morphology of commercial zeolite by planetary ball mill. Advanced Materials Research, 795: 711-715.

Mullin, J.W. 2001. Crystallization (4th Edition), Elsevier, London.

Navarro, E., Baun, A., Behra, R., Hartmann, N.B., Filser, J., Miao, A.J., Quigg, A., Santschi, P.H., and Sigg, L. 2008. Environmental behavior and ecotoxicity of engineered nanoparticles to algae, plants and fungi. Ecotoxicology, 17: 372-386.

Nicole, J., Binata, R., Koodali, T., and Ranjit, C. 2008. Antibacterial activity of ZnO nanoparticle suspensions on a broad spectrum of microorganisms. FEMS Microbiology Letters, 279: 71-76.

Padmavathy, N., and Vijayaraghavan, R. 2008. Enhanced bioactivity of ZnO nanoparticles - an antibacterial study. Science and Technology of Advanced Materials, 9: 1-7.

Padmavathy, N., and Vijayaraghavan, R. 2011. Interaction of ZnO nanoparticles with microbes – a physio and biochemical assay. Journal of Biomedical Nanotechnology, 7: 813-822.

Peck, R.K., Kim, J.M., Choi, Y.J., Kim, S.H., Kang, I.C., Cho, K.Y., Park, W.D., Lee, J.H., Lee, S.M., and Ko, S.K. 2012. In vitro time-kill studies of antimicrobial agents

against blood isolates of imipenem-resistant *Acinetobacter baumannii*, including colistin- or tigecycline- resistant isolates. Journal of Medical Microbiology, 61: 353-360.

Reddy, K. M., Feris, K., Bell, J., Wingett, D. G., Hanley, C., and Punnoose, A. 2007. Selective toxicity of zinc oxide nanoparticles to prokaryotic and eukaryotic systems. Applied Physics Letters, 90: 213902-213903.

Saldamli, I., Kokshel, H., Ozboy, O., Ozalp, I., and Kilic, I. 1996. Zinc supplemented bread and its utilization in zinc deficiency. Cereal Chemistry, 73: 424-427.

Sawai, J. 2003. Quantitative evaluation of antibacterial activities of metallic oxide powders (ZnO, MgO and CaO) by conductimetric assay. Journal of Microbiological Methods, 54: 177-182.

Sawai, J., Shoji, S., Igarashi, H., Hashimoto, A., Kokugan, T., Shimizu, M., and Kojima, H. 1998. Hydrogen peroxide as an antibacterial factor in zinc oxide powder slurry. Journal of Fermentation and Bioengineering, 86: 521–522.

Schmidt-Mende, L., and MacManus-Driscoll, J.L. 2007. ZnO – nanostructures, defects, and devices. Materials Today, 10: 40-48.

Shah, N. S., Ali, I. S., Ali, R. S., Naeem, M., Bibi, Y., Ali, R. S., Raza, M. S., Khan, Y., and Sherwani, K. S. 2016. Synthesis and characterization of zinc oxide nanoparticles for antibacterial applications. Journal of Basic and Applied Sciences, 12: 205-210.

Shakerimoghaddam, A., Ghaemi, E. A., and Jamalli, A. 2017. Zinc oxide nanoparticle reduced biofilm formation and antigen 43 expressions in uropathogenic *Escherichia coli*. *Iran* Journal of *Basic* Medical Sciences, 20: 451-456.

Shi, L.E., Li, Z.H., Zheng, W., Zhao, Y.F., Jin, Y.F., and Tang, Z. X. 2014. Synthesis, antibacterial activity, antibacterial mechanism and food applications of ZnO nanoparticles: a review. Food Additives and Contaminants: Part A; 31: 173-186.

Siddiquah, A., Hashmi, S.S., Mushtaq, S., Renouard, S., Blondeau, J.P., Abbasi, R., Hano, C., Abbasi, B.H. 2018. Exploiting *in vitro* potential and characterization of surface modified Zinc oxide nanoparticles of *Isodon rugosus* extract: Their clinical potential towards HepG2 cell line and human pathogenic bacteria. EXCLI Journal, 17: 671-687.

Sirelkhatim, A., Mahmud, S., Seeni, A., Kaus, N.H.M., Ann, L.C., Bakhori, S.K.M., Hasan, H., and Mohamad, D. 2015. Review on zinc oxide nanoparticles: Antibacterial activity and toxicity mechanism. Nano-Micro Letters, 7: 219-242.

Soosen Samuel, M., Bose, L., and George, K.C. 2009. Optical properties of ZnO nanoparticles. Academic Review, 16: 57-65.

Stoimenov, P.K., Klinger, R.L., Marchin, G.L., and Klabunde, K.J. 2002. Metal oxide nanoparticles as bactericidal agents. Langmuir, 18: 6679-6686.

Swaroop, K., and Somashekarappa, M.H. 2015. Effect of pH values on surface morphology and particle size variation in ZnO nanoparticles synthesised by co-precipitation method. Research Journal of Recent Sciences, 4: 197-201.

Tam, K.H., Djurisic, A.B., Chan, C.M.N., Xi, Y.Y., Tse, C.W., Leung, Y.H., Chan, W.K., Leung, F.C.C., and Au, D.W.T. 2008. Antibacterial activity of ZnO nanorods prepared by a hydrothermal method. Thin Solid Films, 516: 6167-6174.

Tayel, A.A., El-Tras, F.W., Moussa, S., EL-Baz, F.A., Mahrous, H., Salem, F.M., and Brimer, L. 2011. Antibacterial action of zinc oxide nanoparticles against foodborne pathogens. Journal of Food Safety, 31: 211-218.

Uzun, R. O. and Durmuş, H. 2016. Effect of mill type on morphology of AA6013 aluminium powder.revista Matéria, 21: 647-655.

Vani, C., Sergin G.K., and Annamalai, A. 2011. A study on the effect of zinc oxide nanoparticles in *Staphylococcus aureus*. International Journal of Pharma and Bio Sciences, 2: 4326-4335.

Vaseem, M., Umar, A., Hahn, Y.B. 2010. ZnO nanoparticles: Growth, properties, and applications. In: A. Umar and Y.B. Hahn (Eds.), MetalOxide Nanostructures and Their Applications, Chapter 4 (pp. 1-36). New York: American Scientific Publishers.

Wang, Y., Zhang, C., Bi, S., Luo, G. 2010.

Preparation of ZnO nanoparticles using the direct precipitation method in a membrane dispersion micro-structured reactor. Powder Technology, 202: 130-136.

Wang, Z.L. 2004. Zinc oxide nanostructures: growth, properties and applications. Journal of Physics: Condensed Matter, 16: R829–R858, https://doi.org/10.1088/0953-8984/16/25/R01.

Xie, Y., He, Y., Irwin, L.P., Jin, T., and Shi, X. 2011. Antibacterial activity and mechanism of action of zinc oxide nanoparticles against *Campylobacter jejuni*. Applied and Environmental Microbiology, 77: 2325-2331.

Yang, H., Liu, C., Yang, D., Zhang, H., and Xi, Z. 2009. Comparative study of cytotoxicity, oxidative stress and genotoxicity induced by four typical nanomaterials: The role of particle size, shape and composition. Journal of Applied Toxicology, 29: 69-78.

Yu, J., Zhang, W., Li, Y., Wang, G., Yang, L., Jin, J., Chen, Q., and Huang, M. 2004. Synthesis, characterization, antimicrobial activity and mechanism of a novel hydroxyapatite whisker/nano zinc oxide biomateriali. Biomedical Material, 10: doi: 10.1088/1748-6041/10/1/015001.

Yusof, H.M, Mohamad, R., Zaidan, U.H., and Abdul Rahman, N'A. 2019. Microbial synthesis of zinc oxide nanoparticles and their potential application as an antimicrobial agent and a feed supplement in animal industry: a review. Journal of Animal Science and Biotechnology, 10: 57, https://doi.org/10.1186/s40104-019-0368-z.

Yuvakkumar, R., Suresh, J., Saravanakumar, B., Nathanaeld, A.J., and Honga, S.I.R. 2015. Rambutan peels promoted biomimetic synthesis of bioinspired zinc oxide nanochains for biomedical applications. Spectrochimica Acta Part A: Molecular and Biomolecular Spectroscopy, 137: 250-258.

Zhang, L., Ding, Y., Povey, M., and York, D. 2008. ZnO nanofluids – a potential antibacterial agent. Progress in National Science, 18: 939–944.

Zhang, L., Jiang, Y., Ding, Y., Povey, M., and York, D. 2007. Investigation into the antibacterial behaviour of suspensions of ZnO nanoparticles (ZnO nanofluids). Journal of Nanoparticle Research, 9: 479-489.

Zhou, G., Liu, H., He, J., Yuan Y., and Yuan, Z. 2008. The occurrence of *Bacillus cereus*, *B. thuringiensis* and *B. mycoides* in Chinese pasteurized full fat milk. International Journal of Food Microbiology, 121: 195-200.

**How to cite this article:**

Anjie Jamal, Ramadan Awad and Hoda Yusef. 2019. Evaluation of Antimicrobial Activity of ZnO Nanoparticles against Foodborne Pathogens. *Int.J.Curr.Microbiol.App.Sci.* 8(11): 2000-2025. doi: https://doi.org/10.20546/ijcmas.2019.811.234